NUMERICAL STUDY ON THE EFFECTS OF VANE ANGLE AND DIMPLE ON THE THERMAL HYDRAULIC PERFORMANCE OF A PWR FUEL ASSEMBLY

Hui Zhang, Bao-Wen Yang, Bin Zhang*, Bin Han
Science and Technology Center for Advanced Fuel Research & Development, School of Nuclear Science and Technology, Xi'an Jiaotong University
Xianning West Rd. 28, Xi'an, Shaanxi 710049, P.R. China
binzhang@mail.xjtu.edu.cn

Yanping Huang
CNNC Key Laboratory on Nuclear Reactor Thermal Hydraulics Technology
Nuclear Power Institute of China, Chengdu, 610041, China

ABSTRACT

As the most important structure to enhance fuel assembly CHF and increase economic efficiency of reactors, mixing vane spacer grids have always been the focus of numerical simulations and experimental studies. Currently, the design of commercial mixing vane grids strongly depends on full-scale thermal hydraulic experiments, which are expensive and time consuming. With the recent development of computer technology, numerical studies using computational fluid dynamics (CFD) have been conducted to enhance the understanding and design of commercial mixing vane grids. In current numerical simulations of spacer grid mixing effect, most researchers do not distinguish the impact from different components, but look to encompass all component effects of the entire spacer grid including those of vanes, dimples, springs, and straps for their overall mixing performance. In this paper, two spacer grids were modeled to obtain the effects of the mixing vane and dimple respectively. Four grids of different vane angles and three grids of different dimple shapes were examined. First, the effect of vane angle was examined using four different grids of different vane angles without the presence of dimples or spring. Then, both mixing vanes and dimples were added to the grids in order to investigate the compound mixing effects caused by dimples with the presence of mixing vane. During this series of study, the dimple shape was changed while keeping the vane angle fixed. Two different commercial codes, CFX and STAR-CD, were applied to study the flow field under the same operating conditions to provide code-to-code benchmarking. As a basic verification, the results of CFD simulated pressure drop were compared against experimental data. Relatively good agreement between the experimental and simulated pressure drops was obtained. Code to code comparison indicated that different CFD codes provide similar results with slight variations. Further work is needed with more experimental data to verify the turbulence effects and benchmark the CFD results under various thermal hydraulic conditions.

KEYWORDS
Vane angle, dimple shape, pressure drop, turbulence model

1. INTRODUCTION

The design of commercial mixing vane grids strongly depends on the experienced trial and error method and the expensive full-scale thermal hydraulic experiments. As the CFD technology is widely applied in the analyses of nuclear reactor thermal-hydraulic, CFD numerical simulation research has been done to obtain the complex flow field and non-uniform temperature field in nuclear engineering [1-5]. The grid models used in most current studies origin from nuclear plant spacer grids, such as AFA-2G, AFA-3G, OFA and RFA. In current studies, most researchers encompass all component effects of the entire spacer grid including those of vanes, dimples, springs, and straps for their overall mixing performance. This may lead to the lumped parameters effect. From the point of fundamental research, in this paper two CFD software were used to study individual effect of vane angles and dimple shapes to the flow field, pressure drop of a 5x5 split vane type mixing vane grid. Validation was made by comparing the simulation results against experimental pressure drop data, and an indirect verification was also done by code to code comparison using two different commercial codes.

2. BENCHMARK

A direct and indirect benchmarks have been done by experiment and code to code comparison.

2.1. Experiment Benchmark

Since 1998, Framatome has carried out research on the flow and pressure field downstream of spacer grids with mixing vanes, dimples and springs. In this paper, the pressure drop data is compared to a set of experimental data obtained from a test section with rod bundles contained 8 regular mixing vane grids and 3 intermediate flow mixing devices as well as simple support grids. The grids geometry used in the benchmark work is shown in Fig. 1. Due to the limit of computer computation power, only one single grid span was simulated. The comparison results between pressure drop and experimental data are shown in Table I and Table II.

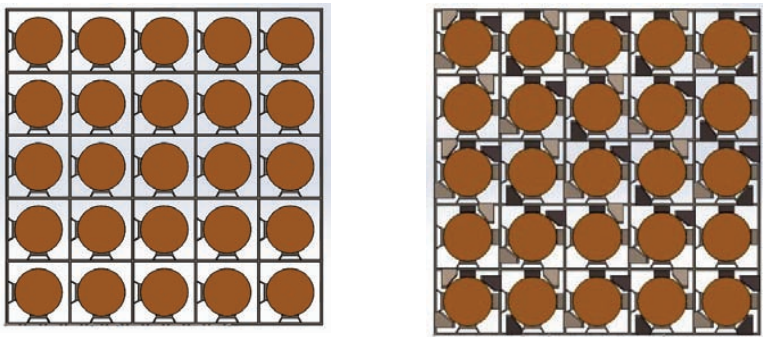

(a)Support vaneless spacer grid **(b)Mixing vane spacer grid**

Fig 1. Benchmark grid geometry

Table I shows the experiment working conditions and Table II shows that the relative error between experiment and calculation results. For the restriction of computational resources, only one mixing vane (MV) grid and simple support (SS) grid was modeled in the simulation. And the equivalent pressure drop data is half of the experiment pressure drop data which contained two MV grids and two SS grids. The maximum deviation of the CFD model is 10%. The differences may be caused by the simplification of the grid geometry, the application of single grid span to replace the full-scale span, and the equivalent of experimental data. In four turbulence models, the Baseline(BSL) Reynolds Stress Model obtained the minimum relative error because interpolation method was adopted in the BSL model to obtain coefficients of the ω–equation, as well as the turbulent Prandtl numbers.

Table I Experimental condition and data

System pressure (MPa)	Temperature (℃)	Inlet velocity (m/s)	Equivalent experiment data (Pa)
6.998	27.5	2.06	12479.5

Table II CFX calculation comparison

Turbulence model	Equivalent experiment data (Pa)	CFX calculation data (Pa)	Relative error %
k-ε	12479.5	11710.4	5.96
RNG k-ε	12479.5	11420.3	8.68
SSG Re	12479.5	11318.0	9.31
BSL Re	12479.5	12313.1	1.33

2.2. Code to Code Benchmark

After the experiment benchmark had been done, another indirect benchmark was made as a complement of validation. By using the same mesh grid, turbulence model, and boundary condition, a code to code simulation was conducted by two software (CFX and STAR-CD) to compare and benchmark the CFD results. Fig. 2 gives the lateral velocity difference in 50 mm downstream of the grid by two codes.

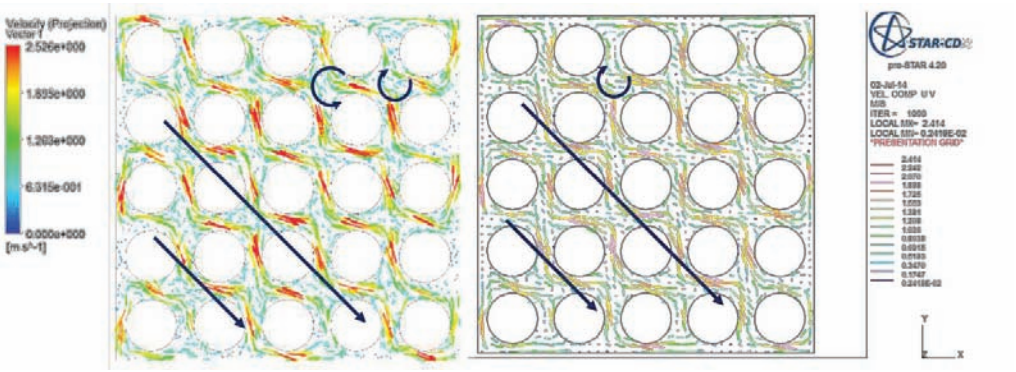

(a) CFX **(b) STAR-CD**

Fig 2. Lateral velocity of different CFD codes at 50 mm downstream of the grid

Fig. 2 shows that the two codes get the same overall flow patterns, which indicates the CFD simulation is reasonable. The lateral velocity vector distribution almost appears to be symmetric, and the max velocity value locates in the gap between bundles. Because the bundle gap is narrower than the center region of subchannels, the fluid would be accelerated in the narrow gap. In the edge of the channel, when fluid

from two directions join together, secondary flow and small eddy will appear in that region. However, two simulation results still have some differences.
Two codes got the similar trend of velocity distribution, however, there are still some differences between the results obtained from these two codes. The maximum velocity appeared in the narrow gap between rods, and the velocity directions in rod gaps are similar between two codes. The calculated max velocity value and secondary flow location are different from two codes. The difference can be caused by many reasons, such as solution methods, material properties setting, CFD model difference, and method sensitivity, etc.

3. CFD SIMULATION MODEL

After the benchmark work, the validated CFD model methods have been used in the vane angle and dimple shape effect simulation. The geometry models and turbulence models are described in next chapters.

3.1. Geometry Model

A split vane type 5x5 mixing vane grid was built as the geometric model, and different components including vane angles and dimple shapes were analyzed separately. The rod diameter is 9.5 mm, the pitch is 12.6 mm, the height of the grid is 33 mm, and the grid length and width are both 63.4 mm. Fig. 3 shows the vane geometry and angle direction.

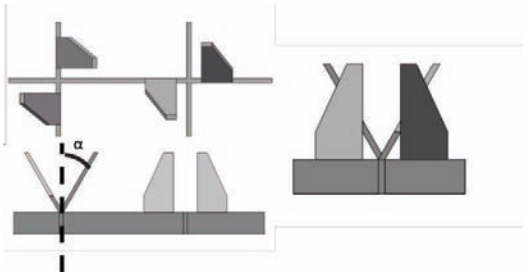

Fig 3. Mixing vane angle and distribution

To obtain the dimple shape influence on flow field, pressure drop, and CHF location, three different dimples were modeled. The dimple shapes are shown in Fig. 4. The streamline type-A dimple and streamline type-B dimple are semi-enclosed and have arc shaped surface which can lead fluid to a specific direction. The traditional type dimple has the strip and opening structure which can only disturb the flow. It cannot divert the flow coherently toward a targeted direction. Fluid can go through the traditional dimple easier than the streamline dimple because of the opening hole.

(a) Streamline type-A (b) Streamline type-B (c) Tradition

Fig 4. Different dimple shapes

3.2. Mesh Strategy

Due to the limitation of computational power, a representative length of a single grid span was chosen as the calculation domain. The domain was divided into three parts, the entrance section, the grid section, and the outlet section. The whole length of the computational domain was 783 mm while the entrance section length was 250 mm and the outlet section was 500 mm. The computational domain geometry was complex so that different mesh strategies had to be applied to three sections separately. The existence of vanes and dimples made it difficult to use hexahedron mesh in grid section, so the automatic tetrahedron mesh was applied in this part. The structured hexahedron mesh is suitable for the upstream and downstream of the spacer grids, so structured mesh is used in the two parts. Mesh independent results were obtained when mesh number reached 13271304(Mesh-2) in CFX. Fig 5.shows the local view of the mesh result. The mesh independent comparison result is shown in Fig 6. In very few points, the max deviation between mesh-2 and mesh-3 is 3.1% and 7.3% separately in pressure drop value and lateral velocity distribution. In most location, the differences between the two meshes are less than 1%. So the mesh-2 is considered as the mesh independent result.

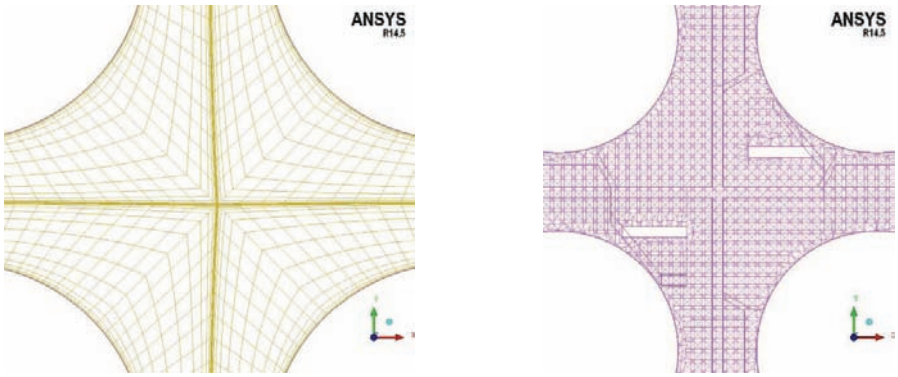

(a) Mesh in the bare rod region (b) Mesh near grid vane region

Fig 5. Mesh cross section local view

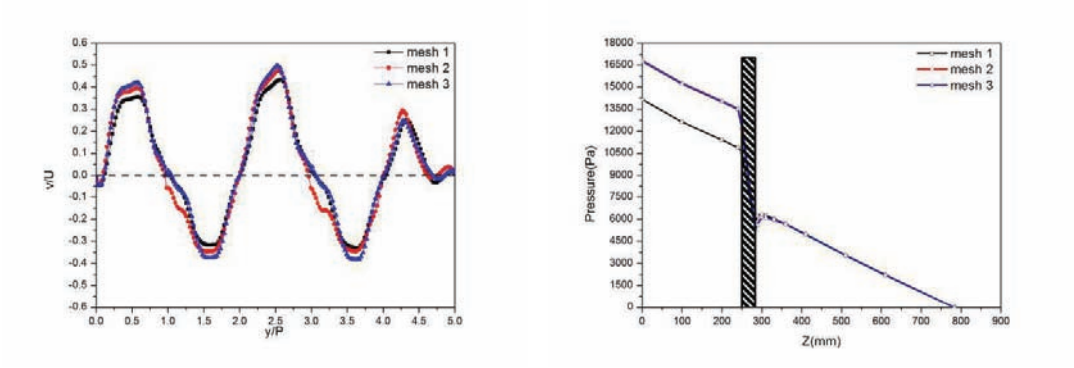

(b) Lateral velocity comparison **(b) Pressure drop comparison**

Fig 6. Mesh independent results

3.3. Simulation Setup

3.3.1 Boundary Condition

The high resolution advection scheme was applied in CFX to discrete equation while in STAR-CD the simple algorithm was used. A monitor plane was set in the 250 mm downstream grid section in the solution process. The max iteration steps were 800 and the residual target was set to be 10^{-5}. The boundary conditions are listed in Table III, and system pressure was set to be 15.5MPa.

Table III

POSITION	BOUNDARY TYPE	VALUE
INLET	Velocity and temperature	4.737m/s 310℃
OUTLET	Relative Pressure	0 Pa
ROD BUNDLE AND GRIDS WALL	Adiabatic and no-slip	

3.3.2 Turbulence model

Periodical mixing induced by spacer grid, interaction between opening subchannels and complexity of turbulence bring about the uncertainty to choose a standard turbulence model. Lots of models have been examined by different researchers [6-10], such as *k-ε*, *k-ω*, RNG *k-ε*, SST, SSG, LES, etc.

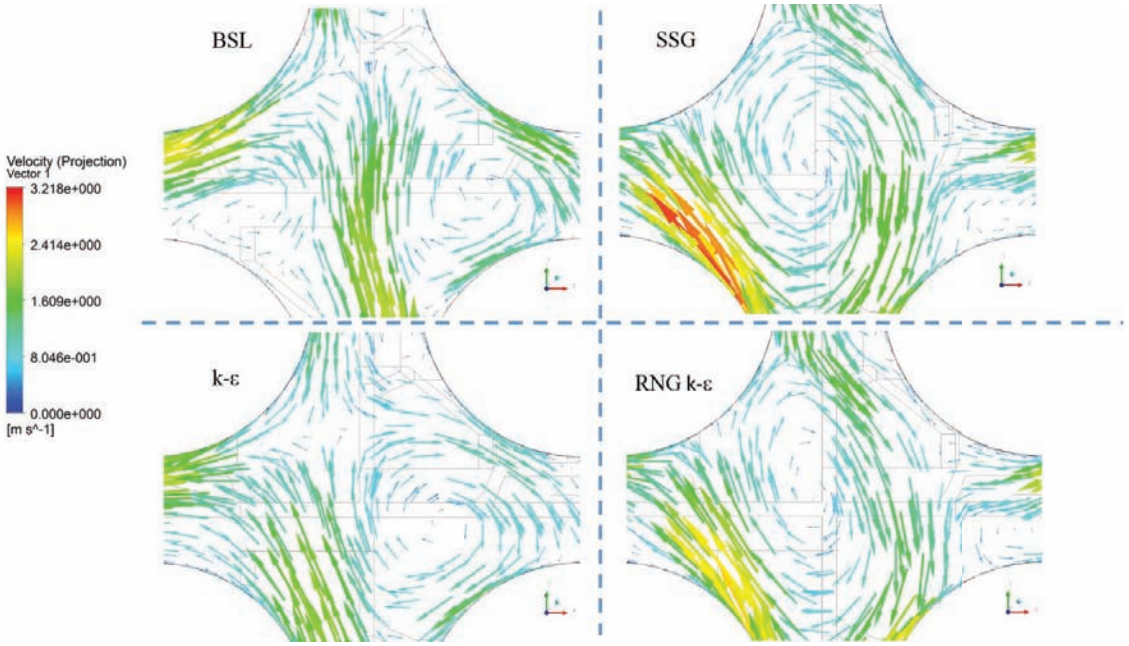

Fig 7. Comparison of lateral velocity vector of four turbulence models in 110mm downstream of the Streamline type-A dimple grid

Fig 7. shows the local flow field nearby the rods of streamline dimple grids which was obtained by four turbulence models. The figure indicates that different turbulence models can lead to the variation of flow field downstream the grid. More small eddies can be observed from BSL turbulence mode results. That phenomenon may demonstrated a better prediction of secondary flow can be made by BSL Reynolds Stress model. Besides, the previous validation results shows that BSL Reynolds Stress model with a minimum relative error comparing to experimental pressure drop data, so this turbulence model was used in the study of vane angle and dimple effect.

4. RESULT

4.1. The Effect of Mixing Vane Angle on Pressure Drop

A split vane type grid with different angles (around 29°) were simulated and analyzed in this paper. Usually lateral velocity and pressure drop tend to increase with the increase in vane angle. Figure. 8 shows the pressure drop along the axial direction of different angles.

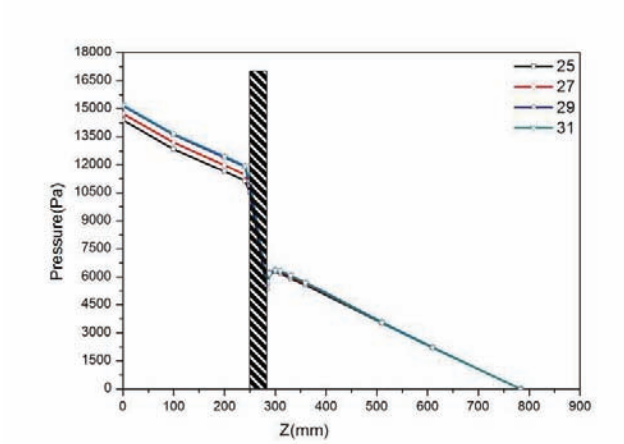

Figure 8. Pressure drop along the axial direction of different mixing vane angles

With the increase of vane angles, the distinction of pressure distribution tends to increase. The deviation of pressure drop is no more than 3% due to the similar projected area in axial direction of four angles. Lowest pressure drop was obtained when the vane angle was 25° due to its minimum axial projected area. The pressure drop difference between 29° and 31° is small. Fig. 9 shows the pressure distribution of four vane angles at downstream section of the grids.

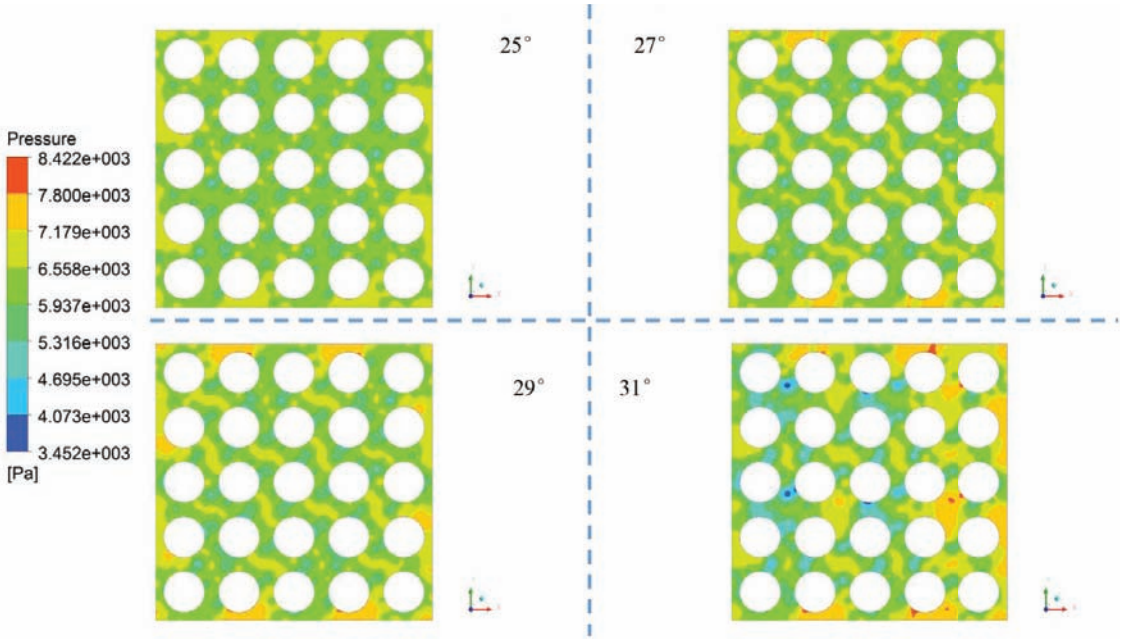

Fig 9. Pressure contours of 25° 27° 29° and 31° at 50mm downstream of the grid

Four picture contours are compared under the same variation range. The red region is the high pressure area, while the blue region is the low pressure area. The difference between max and min pressure is 5000 Pa. Obviously, the pressure field stability and directivity of 25° vane angle is worse than 29°. Axial pressure drop of the 29° grid was not the smallest, but an optimal balance between stable capacity and pressure drop was obtained.

4.2. The Effect of Dimple Shape on Pressure Drop and Flow Field

The mixing effect induced by spacer grids largely depends on the mixing vane, so the grid thermal-hydraulic performance can be improved by enhancing the vane mixing ability. When the total flow flux is constant, if the fluid flow to the mixing vane in the proper direction, the mixing effect can be improved. By changing dimple shapes, the dimple can be made to contain the guiding flow function, which leads the fluid to the mixing vane and increases the thermal-hydraulic performance of grids. Simulations have been done under the three different dimples shown in Fig. 4.

4.2.1. Dimensionless velocity comparison

Define expression: v/U as the dimensionless velocity in Y direction. U is the inlet axial velocity, and v is the lateral velocity in Y direction. Similarly, the expression y/P represents the dimensionless length in Y direction. P is the rod bundle pitch.

As shown in Fig. 10, the dimensionless lateral velocity decreases with the increase of axial height. The trend was caused by the dispersion of mixing effect in the position further downstream of the grid section. In upstream of the grid, the lateral dimensionless velocity is nearly 0 because of the absence of mixing vanes and dimples. As the fluid flows through the grid region, and the vanes and dimples interact with the fluid, the mixing effect increases. So in the near grid downstream region, for example, at 50 mm distance from the grid, the dimensionless X and Y velocity became larger and demonstrating symmetric distribution in zero axial. In the half grid span and single grid span position, the variation of dimensionless velocity became small and irregular. This may be caused by the complicated environment in rod bundles.

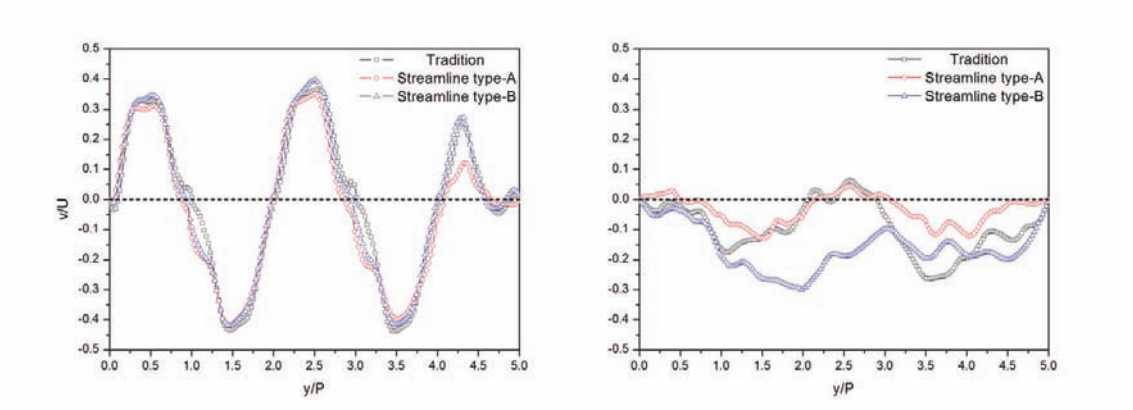

(a) 50 mm downstream of spacer grids **(b) 250 mm downstream of spacer grids**

Fig 10. Dimensionless velocity at different height of three dimples

Besides, in the downstream region away from spacer grid, turbulent mixing and cross flow mixing from different subchannels in different directions may lead to irregular distribution phenomenon. Fig. 10 shows the different dimensionless velocity of three dimples at two different axial heights in a certain channel. The dimensionless velocity difference between various dimples becomes large in further downstream location.

4.2.2. Lateral velocity comparison

Fig. 11 gives the lateral velocity vectors distribution of three dimples at 250 mm downstream of the grid. It is known from that 110 mm downstream of the grid, the lateral velocity of three different dimples are always same. The major mixing effect is caused by the mixing vane, and the dimple shape is not important at location near the mixing vane region. As the flow travel further to 250 mm downstream of

the grid, the effect of dimples becomes obvious. As the flow travel beyond 250 mm away from the mixing vane grid, the effect of dimple shapes on the lateral velocity become more significant. This phenomenon also exists in local flow field.

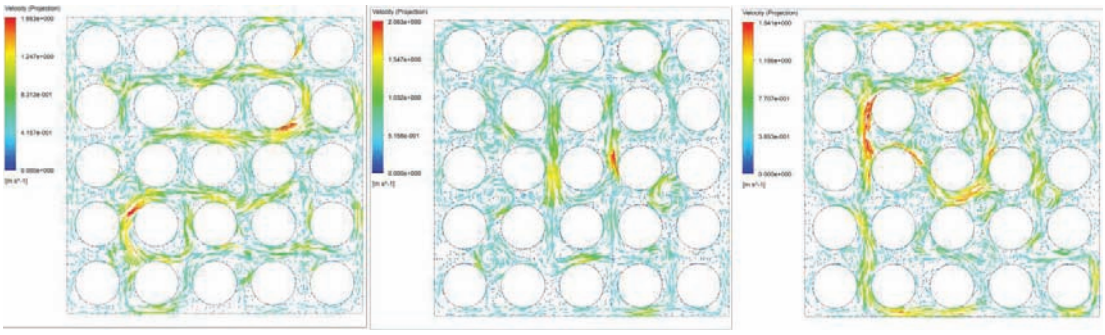

Tradition **Streamline type-A** **Streamline type-B**

Fig 11. Lateral velocity at 250 mm downstream of the grid

4.2.3. Pressure drop comparison

Fig. 12 shows the variation of pressure plotted against the axial height for three different dimples. The pressure drop of the traditional dimple is the lowest. The projection area of the tradition dimple the streamline type-A dimple and streamline-B dimple are 2.35 mm^2, 8.43 mm^2 and 4.56mm^2 respectively. It is known to all that the projection area of tradition dimple is smaller than the other two streamline dimples, which leads to the low flow resistance result.

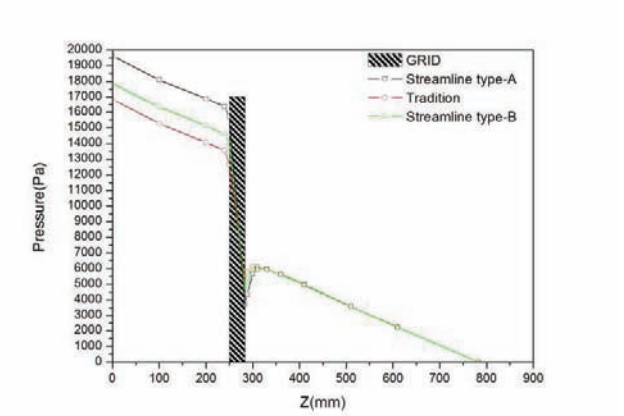

Fig 12. Pressure drop along the axial direction of three type dimples

At the immediate downstream of the mixing grid, the pressure drop of three different dimples are almost the same. As the flow passing the mixing vane grid, the local pressure increases first then decreases linearly. The pressure increase is caused by the sudden decrease of the axial projection blockage area due to mixing vane at downstream of the grid. At the crossing of the mixing vane grid, the average velocity increases with the increase of projection area, which brings about the increase of pressure drop.

5. CONCLUSIONS

Appropriate CFD models have been validated by direct benchmark with experiment data and indirect

benchmark with code to code comparison. Simulations have been done to study the vane angles and dimple shape effect to flow field and pressure drop. The effects of these two components can be summarized as follows:

- Near the mixing vane region, the lateral velocity is proportional to the mixing vane angle; however, the pressure field of mixing vane with 29° is the most stable. Although the pressure drop of 29° is larger than that of 25°, 29° mixing vane can get a better balance between lateral velocity and pressure drop.
- The dimple shape effect can play the major role in further distance downstream of the grid, but pressure drop of the two streamline dimples are larger than traditional dimple. More to be done on dimple shapes to get the optimal dimple.

6. ACKNOWLEDGE

This work is performed as a joint research project between Xi'an Jiaotong University and CNNC Key Laboratory on Nuclear Reactor Thermal Hydraulics Technology

REFERENCES

1. ByungSoo Shin, Soon Heung Chang, "CHF experiment and CFD analysis in a 2×3 rod bundle with mixing vane," *Nuclear Engineering and Design*, **239**; pp. 899–912 (2009)
2. Ikeda K, Makino Y, Hoshi M, "Single phase CFD applicability for estimating fluid hot-spot locations in a 5× 5 fuel rod bundle," *Nuclear Engineering and Design*, **236**(11), pp. 1149-1154(2006).
3. C.M. Lee, Y.D. Choi, "Comparison of thermo-hydraulic performances of large scale vortex flow (LSVF) and small scale vortex flow (SSVF) mixing vanes in 17×17 nuclear rod bundle," *Nuclear Engineering and Design*, **237**, pp. 2322–2331(2007).
4. M. E. Connera, E. Baglietto, A. M. Elmahdia, CFD methodology and validation for single-phase flow in PWR fuel assemblies, *Nuclear Engineering and Design*, **240** (2010) 2088–2095.
5. M. A. Navarro, A. A. C. Santos, "Evaluation of a numeric procedure for flow simulation of a 5×5 PWR rod bundle with a mixing vane spacer," Progress in Nuclear Energy, **53**, pp.1190-1196 (2011).
6. Bieder U, Falk F, Fauchet G, "LES analysis of the flow in a simplified PWR assembly with mixing-grid," *Progress in Nuclear Energy*, **75**, pp.15-24(2014).
7. Bakosi J, Christon M A, Lowrie R B, et al, "Large-eddy simulations of turbulent flow for grid-to-rod fretting in nuclear reactors," *Nuclear Engineering and Design*, **262**, pp.544-561(2013).
8. Cinosi, N., et al, "CFD simulation of turbulent flow in a rod bundle with spacer grids (MATIS-H) using STAR-CCM+," *Nuclear Engineering and Design*, 279, pp.37-49(2014).
9. Tseng Y S, Ferng Y M, Lin C H, "Investigating flow and heat transfer characteristics in a fuel bundle-with split-vane pair grids by CFD methodology," *Annals of Nuclear Energy*, **64**, pp.93-99(2014).
10. Yan J, Zhang Y, Yang B, et al, "Influence of Spacer Grid Outer Strap on Fuel Assembly Thermal Hydraulic Performance," *Science and Technology of Nuclear Installations*, (2014).